Supplementary Material of "Theory of Droplet Ripening in Stiffness Gradients"

Estefania Vidal-Henriquez and David Zwicker
Max-Planck Institute for Dynamics and Self-Organization, Am Faßberg 17, 37077 Göttingen, Germany.
(Dated: June 2, 2020)

I. EQUILIBRIUM CONCENTRATIONS IN THE PRESENCE OF EXTERNAL PRESSURE

To understand the system presented in the main manuscript we describe a two-phase system and aim to obtain the change in the equilibrium concentrations when an external pressure is added to the droplet. For a demixed system to be stable, the dilute and the droplet phase need to reach an equilibrium in both chemical potential and osmotic pressure. Assuming an infinite system and given the free energy density of the system $f(V, P, \phi)$, the equilibrium volume fractions in the droplet and dilute phase, $\phi^0_{\rm in}$ and $\phi^0_{\rm out}$, respectively, fulfil the relations [2],

$$0 = f'(\phi^0_{\rm out}) - f'(\phi^0_{\rm in}) \qquad \text{and} \tag{S.1a}$$

$$0 = f(\phi^0_{\rm in}) - f(\phi^0_{\rm out}) + (\phi^0_{\rm out} - \phi^0_{\rm in}) f'(\phi^0_{\rm out}), \tag{S.1b}$$

where the free energy density is differentiated with respect to the volume fraction. Note that for clarity we used here a slightly different notation than in the main manuscript. The expressions $\phi^{\rm eq}_{\rm out}$, $\phi^0_{\rm out}$, and $\phi^{\rm eq}_{\rm in}$ here used, correspond to $\phi_{\rm eq}$, ϕ_0, and $\phi_{\rm in}$ in the main manuscript, respectively. These equations can be solved using a Maxwell construction as shown in Figure S.1 (purple dotted line). Analogously, when there is a pressure jump P at the interface between phases the new equilibrium concentrations $\phi^{\rm eq}_{\rm in}$ and $\phi^{\rm eq}_{\rm out}$ reach a pressure balance,

$$0 = f(\phi^{\rm eq}_{\rm in}) - f(\phi^{\rm eq}_{\rm out}) + (\phi^{\rm eq}_{\rm out} - \phi^{\rm eq}_{\rm in}) f'(\phi^{\rm eq}_{\rm out}) + P. \tag{S.2}$$

The change in equilibrium concentration due to P can be seen in the corresponding Maxwell construction of this system, shown in Figure S.1 (red continuous lines). If the dense phase is tightly packed the molecules can not compress further and thus $f(\phi^{\rm eq}_{\rm in}) \approx f(\phi^0_{\rm in})$. Using this approximation, Eqs. (S.1b) and (S.2) can be combined as follows

$$0 = f(\phi^0_{\rm out}) - f(\phi^{\rm eq}_{\rm out}) - (\phi^0_{\rm out} - \phi^0_{\rm in}) f'(\phi^0_{\rm out}) + (\phi^{\rm eq}_{\rm out} - \phi^{\rm eq}_{\rm in}) f'(\phi^{\rm eq}_{\rm out}) + P. \tag{S.3}$$

Assuming that the pressure increase produces a small change in concentration we can approximate the free energy at the new volume fraction up to first order,

$$f(\phi^{\rm eq}_{\rm out}) \approx f(\phi^0_{\rm out}) + f'(\phi^0_{\rm out})(\phi^{\rm eq}_{\rm out} - \phi^0_{\rm out}) \,. \tag{S.4}$$

With this approximation and using $\phi^{\rm eq}_{\rm in} \approx \phi^0_{\rm in}$, Eq. (S.3) reduces to

$$0 = (\phi^{\rm eq}_{\rm out} - \phi^{\rm eq}_{\rm in}) \left[f'(\phi^{\rm eq}_{\rm out}) - f'(\phi^0_{\rm out}) \right] + P \,. \tag{S.5}$$

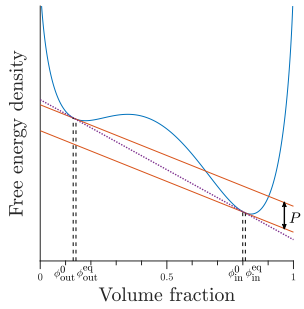

FIG. S.1. Maxwell construction showing the equilibrium volume fraction of the droplet phase, $\phi^0_{\rm in}$, and dilute phase, $\phi^0_{\rm out}$, in the absence of external pressure, Eq. (S.1) (purple dotted line) and how these equilibrium values shift to $\phi^{\rm eq}_{\rm in}$ and $\phi^{\rm eq}_{\rm out}$ in the presence of a pressure difference P, Eq (S.2) (red continuous lines).

Assuming strong phase separation $\phi^{\rm eq}_{\rm in} \gg \phi^{\rm eq}_{\rm out}$ and using the definition of chemical potential $\mu = \nu f'(\phi)$, where ν is the molecular volume of the phase separating material; we obtain an expression for the change of the chemical potential in the dilute phase, due to a change in pressure,

$$P = c^{\rm eq}_{\rm in} \left[\mu^{\rm eq}_{\rm out} - \mu^0_{\rm out} \right] \tag{S.6}$$

where $c_{\rm in} = \phi_{\rm in}/\nu$ is the material concentration inside the droplets. Finally, assuming an ideal dilute phase we can approximate $\mu(\phi_{\rm out}) \approx k_{\rm B}T \log \phi_{\rm out}$, with $k_{\rm B}$ the Boltzmann constant and T the absolute temperature, and obtain [1]

$$\phi^{\rm eq}_{\rm out} \approx \phi^0_{\rm out} \exp\left(\frac{P}{c_{\rm in} k_{\rm B} T} \right). \tag{S.7}$$

Using the notation of the main manuscript: $\phi^0_{\rm out} = \phi_0$ and $\phi^{\rm eq}_{\rm out} = \phi_{\rm eq}$, Eq. (S.7) is equivalent to Eq. 1 of the main text.

II. DERIVATION OF THE COARSE-GRAINED MODEL

In this section we average over individual droplets and deduce an equation for the volume fraction ψ of the material present in the droplet phase, it is defined as

$$\psi(\vec{x}) = \phi_{\rm in} \frac{\iiint \sum V_i \delta(\vec{x_i} - \vec{x}) dV}{\iiint dV} \,, \tag{S.8}$$

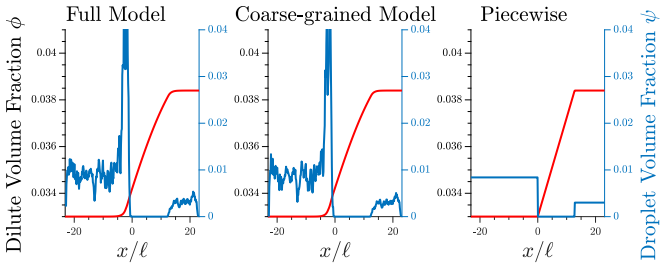

FIG. S.2. Comparison of the three models used in this work (at a late time point): Full Model Equation (Eqs. 4-5), Reduced Model Equation (Eqs. 8), and Piecewise Model Equation S.15

where the integrals are performed over a small volume V used for coarse graining the system. Assuming monodispersity inside such a volume, the average radius $\langle R\rangle$ of the droplets can be approximated by

$$\langle R\rangle^3 \approx \frac{3\psi}{4\pi\phi_{\text{in}} n} \tag{S.9}$$

where $n(\vec{x})$ is the droplet number density, defined as the number of droplets present in each discretization volume divided by V. If the droplets have similar enough size, then they change volume at similar rates and n does not change over time. From the dynamical equation for the radius of the full model (Eq. (4) in the main manuscript) we obtain the growth rate of a droplet of volume V_i

$$\frac{dV_i}{dt} = -\frac{J_i}{\phi_{\text{in}}} = \frac{4\pi D R_i}{\phi_{\text{in}}}\left(\phi - \phi^{\text{eq}}\right) . \tag{S.10}$$

Coarse-graining this equation, we get

$$\partial_t\psi = \frac{4\pi D\left(\phi-\phi^{\text{eq}}\right)}{V}\iiint \sum_i R_i\delta(\vec{x}-\vec{x_i})dV, \tag{S.11}$$

where the integral is again performed over V. It can be approximated by the average radius multiplied by

$$\iiint \sum_i R_i\delta(\vec{x}-\vec{x_i})dV \approx \langle R\rangle V n(\vec{x}) , \tag{S.12}$$

which in turn can be approximated using Eq. (S.9),

$$\partial_t\psi = 4\pi n D\left(\phi-\phi^{\text{eq}}\right)\left(\frac{3\psi}{4\pi\phi_{\text{in}} n}\right)^{1/3} . \tag{S.13}$$

The equation for $\phi(\vec{x},t)$ comes directly from applying the definition of $\psi(\vec{x},t)$ to the dynamical equation for ϕ of the full model (Eq. (5) of the main manuscript), thus yielding the reduced model

$$\partial_t\psi = D\left(\phi-\phi^{\text{eq}}\right)\left(\frac{48\pi^2 n^2\psi}{\phi_{\text{in}}}\right)^{1/3} , \tag{S.14a}$$

$$\partial_t\phi = D\nabla^2\phi - \partial_t\psi , \tag{S.14b}$$

which we use in the main text.

III. EXPERIMENTAL COMPARISON

We used our model to explain the observations of the elastic ripening experiments [1]. Figure S.3 and Figure 2 in the main manuscript highlight that our model captures the details of the experiments quantitatively. To achieved this agreement, we initialized the simulation with experimentally measured droplet positions and radii, resulting in a mean droplet distance of $\ell = 107.7\,\mu\text{m}$. To account for the sharp transition between the two materials, we used an exponentially decaying profile characterized by a length w,

$$E(x) = \begin{cases} (E_{\text{stiff}} - E_{\text{soft}})(1-e^{-x/w}) + E_{\text{soft}} & x > 0 \\ E_{\text{soft}} & x \le 0 , \end{cases}$$

which is illustrated in the left panel of Fig. S.3. The transition length w was the only fitting parameter used to match the dynamics of the dissolution front. The remaining parameters were measured independently [1]: $D = 50\,\mu\text{m/s}^2$, $\zeta = 0.5$, and $n_L k_B T = 11\,\text{MPa}$, implying $\hat{E} = 22\,\text{MPa}$ and the time scale $t_D = 232\,\text{s}$.

IV. DERIVATION OF THE DISSOLUTION FRONT DYNAMICS

Following the arguments given in the main manuscript, we now calculate the front dynamics at late times, where the front invading the stiff side has travelled a distance L which is much bigger than the transition length, $L \gg w$.

In the area devoid of droplets the dynamics reduce to a simple diffusion equation whose boundary conditions are given by ϕ_{eq} on the soft and stiff sides. If the front moves slow enough we can do a steady state approximation and assume that the area devoid of droplets reaches equilibrium quickly compared to the front speed. For a simple domain we can solve the diffusion equation. In particular, if the elasticity gradient is always in the same direction, we obtain a piecewise approximation dividing the system in three parts along the elasticity gradient direction as follows,

$$\psi = \psi_{\text{soft}}, \quad \phi = \phi_{\text{soft}}, \qquad x < 0 \tag{S.15a}$$

$$\psi = 0, \quad \phi = \phi_{\text{soft}} + \frac{x}{L}\Delta\phi, \qquad 0 < x < L \tag{S.15b}$$

$$\psi = \psi_{\text{stiff}}, \quad \phi = \phi_{\text{stiff}}, \qquad x > L, \tag{S.15c}$$

where L is the front position, $\Delta\phi = \phi_{\text{stiff}} - \phi_{\text{soft}}$ with $\phi_{\text{stiff/soft}} = \phi_{\text{eq}}(E_{\text{stiff/soft}})$, $x = 0$ is chosen to match the position where droplets start to grow instead of shrink, and $\psi_{\text{soft/stiff}}$ are the droplet volume fractions after initial growth. A comparison of the volume fractions ϕ and ψ between simulations and the piecewise approximation are shown in Figure S.2. Integrating Eq. (S.14b) over the length of the stiff side yields an equation for the flux at

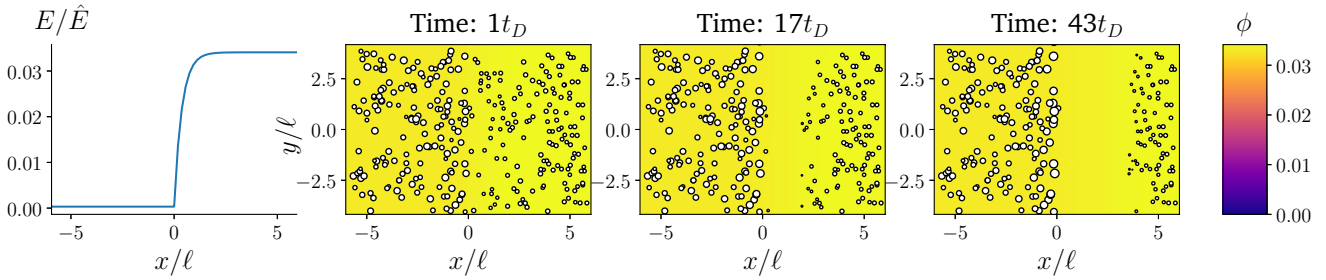

FIG. S.3. Our model quantitatively captures experimental observations of elastic ripening. The stiff region is defined by an elasticity profile (left panel). Subsequent images show projections of 3-dimensional simulations (obtained by solving Eqs. 4–5) of the droplets (symbols) and the volume fraction ϕ in the dilute phase (density plot with color bar on the right) at the indicated times. Model parameters are chosen to match the experiments [1]: $\phi_0 = 0.033$, $\phi_{\text{in}} = 1$, $E_{\text{stiff}} = 0.0341\,\hat{E}$, $E_{\text{soft}} = 3.2 \cdot 10^{-4}\,\hat{E}$, and $w = 0.37\,\ell$. The mean droplet radius on the stiff side is $0.09\,\ell$. The shown data is identical to that of Figure 2 in the main manuscript.

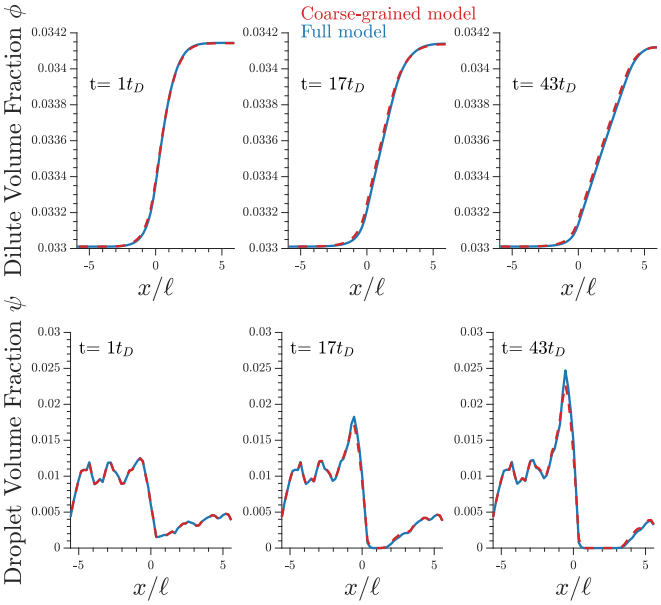

FIG. S.4. The coarse-grained model (Eq. 8 of the main manuscript) captures the behavior of the full model (Eqs. 4-5) in a wide range of parameters. In particular, the volume fractions ϕ in the dilute phase (upper panel) and the droplet volume fractions ψ (lower panel) agree quantitatively for the parameter values used in Figure S.3.

$x = 0$,

$$\partial_t \int_0^L \phi dx + \partial_t \int_L^\infty (\phi + \psi) dx = -D\partial_x(\phi + \psi)|_{x=0} \,. \tag{S.16}$$

Using the piecewise approximation, Eqs. (S.15), the integrals can be easily evaluated, so

$$\partial_t L \frac{\phi_{\text{soft}} + \phi_{\text{stiff}}}{2} - \partial_t L(\phi_{\text{stiff}} + \psi_{\text{stiff}}) = -D\frac{\phi_{\text{stiff}} - \phi_{\text{soft}}}{L} \,.$$

This equation can be rewritten as

$$\partial_t L = \frac{\alpha}{2L} \quad \text{with} \quad \alpha = 4D\left(1 + \frac{2\psi_{\text{stiff}}}{\Delta\phi}\right)^{-1} . \tag{S.17}$$

Finally, solving for L, we find a diffusive motion for the front,

$$L = \sqrt{\alpha(t - t_0)}, \tag{S.18}$$

where t_0 is such that $L(t_0) = 0$. This expression shows that the front moves diffusively, with a speed that increases with the elasticity difference and decreases with higher volume fractions of droplet material ψ. A comparison between this approximation and the measured front speed is presented in the main manuscript.

V. SUPPLEMENTARY VIDEOS

Supplementary video 1: Example of a typical simulation with a one dimensional elasticity gradient. Model parameters are $\phi_0 = 0.033$, $\phi_{\text{in}} = 1$, $\psi_{\text{stiff}} = 0.09\phi_0$, $E_{\text{stiff}} = 0.15\hat{E}$, $E_{\text{soft}} = 10^{-4}\hat{E}$, and $w = 1.4\ell$.

Supplementary video 2: Different visualization of the elastic ripening process. Video showing the radii and position of droplets along with the one dimensional average of the dilute phase over time. Same simulation as in Fig. 1 and Supplementary video 1.

Supplementary video 3: Simulation with a two dimensional sinusoidal elasticity profile. Same parameters as in Fig. 5.

Supplementary video 4: Simulation with a two dimensional elasticity profile in the shape of the Max Planck Society's logo.

[1] Kathryn A Rosowski, Tianqi Sai, Estefania Vidal-Henriquez, David Zwicker, Robert W Style, and Eric R Dufresne. Elastic ripening and inhibition of liquid–liquid phase separation. *Nature Physics*, 16(4):422–425, 2020.

[2] Christoph A Weber, David Zwicker, Frank Jülicher, and Chiu Fan Lee. Physics of active emulsions. *Reports on Progress in Physics*, 82(6):064601, 2019.